RSC Advances

PAPER

View Article Online
View Journal | View Issue

Cite this: *RSC Adv.*, 2023, **13**, 10757

Potential role of a novel biphenanthrene derivative isolated from *Aerides falcata* in central nervous system diseases†

Bachtiar Rivai,[a] Hasriadi,[b] Peththa Wadu Dasuni Wasana,[c] Chaisak Chansriniyom,[de] Pasarapa Towiwat,[bf] Yanyong Punpreuk,[g] Kittisak Likhitwitayawuid,[d] Pornchai Rojsitthisak[fh] and Boonchoo Sritularak[*df]

Central nervous system (CNS) diseases are a significant health burden globally, with the development of novel drugs lagging behind clinical needs. Orchidaceae plants have been traditionally used to treat CNS diseases, leading to the identification of therapeutic leads against CNS diseases from the *Aerides falcata* orchid plant in the present study. The study isolated and characterized ten compounds, including a previously undescribed biphenanthrene derivative, Aerifalcatin (**1**), for the first time from the *A. falcata* extract. The novel compound **1** and known compounds, such as 2,7-dihydroxy-3,4,6-trimethoxyphenanthrene (**5**), agrostonin (**7**), and syringaresinol (**9**), showed potential activity in CNS-associated disease models. Notably, compounds **1**, **5**, **7**, and **9** demonstrated the ability to alleviate LPS-induced NO release in BV-2 microglial cells, with IC_{50} values of 0.9, 2.5, 2.6, and 1.4 μM, respectively. These compounds also significantly inhibited the release of pro-inflammatory cytokines, IL-6 and TNF-α, reflecting their potential anti-neuroinflammatory effects. Additionally, compounds **1**, **7**, and **9** were found to reduce cell growth and migration of glioblastoma and neuroblastoma cells, indicating their potential use as anticancer agents in the CNS. In summary, the bioactive agents isolated from the *A. falcata* extract offer plausible therapeutic options for CNS diseases.

Received 2nd March 2023
Accepted 29th March 2023

DOI: 10.1039/d3ra01402a

rsc.li/rsc-advances

Introduction

Central nervous system (CNS) diseases, encompassing a range of conditions from stroke and neurodegenerative diseases to chronic pain, schizophrenia, and cancer, pose a considerable burden on global public health and the economy. These conditions are associated with high rates of mortality and disability worldwide, particularly in developing countries.[1,2] One in nine individuals suffers and dies from CNS diseases, and the prevalence of CNS diseases remains high and is projected to increase significantly in the future.[1,2] However, current treatments often fall short of meeting clinical needs, and the development of novel therapeutics is stagnant.[3] Consequently, compared to drugs for other conditions, only a few CNS drugs have recently gained approval.[3,4]

The molecular and cellular complexity of CNS diseases is a major impediment to the development of effective drugs.[3] Neuroinflammation has been identified as a crucial contributor to various neurological disorders within the CNS.[4] As a result, neuroinflammation has emerged as a therapeutic target for many CNS diseases, including neurodegenerative disorders, brain injuries, and brain infections.[5–7] In addition to neurological disorders, CNS tumors, such as glioblastoma and primary CNS neuroblastoma, are also characterized by their high complexity, low survival, and poor prognosis.[8] Primary CNS neuroblastoma is a complex disease with limited treatment options due to the lack of understanding of the disease pathophysiology.[9] Therefore, there is a pressing need to discover novel and highly effective pharmacological agents for the treatment of CNS disorders, including neuroinflammation-associated diseases and brain tumors.

[a]*Pharmaceutical Sciences and Technology Program, Faculty of Pharmaceutical Sciences, Chulalongkorn University, Bangkok 10330, Thailand*

[b]*Department of Pharmacology and Physiology, Faculty of Pharmaceutical Sciences, Chulalongkorn University, Bangkok 10330, Thailand*

[c]*Department of Pharmacy, Faculty of Allied Health Sciences, University of Ruhuna, Galle 80000, Sri Lanka*

[d]*Department of Pharmacognosy and Pharmaceutical Botany, Faculty of Pharmaceutical Sciences, Chulalongkorn University, Bangkok 10330, Thailand. E-mail: boonchoo.sr@chula.ac.th*

[e]*Natural Products and Nanoparticles Research Unit, Chulalongkorn University, Bangkok, 10330, Thailand*

[f]*Center of Excellence in Natural Products for Ageing and Chronic Diseases, Chulalongkorn University, Bangkok, 10330, Thailand*

[g]*Department of Agriculture, Ministry of Agriculture and Cooperatives, Bangkok, 10900, Thailand*

[h]*Department of Food and Pharmaceutical Chemistry, Faculty of Pharmaceutical Sciences, Chulalongkorn University, Bangkok 10330, Thailand*

† Electronic supplementary information (ESI) available. See DOI: https://doi.org/10.1039/d3ra01402a

Orchids have been traditionally used in various countries as a remedy for diseases related to the CNS, and recent studies have shown that several orchid species have promising health benefits in the treatment of such diseases.[10,11] For example, *Gastrodia elata* Bl. and *Cypripedium elegans* Rchb. F. have been found to exhibit hypnotic, sedative, and anti-epileptic effects, while *Cypripedium parviflorum* Salisb. has been empirically used to treat insomnia and anxiety.[11] *Dendrobium nobile* Lindl. has been found to be effective in treating neurodegenerative diseases, such as Alzheimer's and Parkinson's diseases, while *Dendrobium moniliforme* (L.) Sw. has been found to inhibit the growth of human brain tumor cells.[12,13] In addition, bioactive compounds isolated from these plants, such as batatasin III from *Dendrobium scabrilingue* Lindl.[14] and protocatechualdehyde from *Dendrobium nobile* Lindl.,[15] have been shown to effectively attenuate CNS diseases, such as neuroinflammation, and erianin from *Dendrobium chrysotoxum* Lindl.[16] and denbinobin from *Dendrobium moniliforme* (L.) Sw.[17] have been found to be effective in the treatment of glioblastoma. Therefore, orchid species and their active compounds have great potential as pharmacological agents in the treatment of CNS diseases.

Aerides falcata Lindl. & Paxton, commonly known as "Ueng Kulaab Krapao Perd" in Thailand (Fig. 1A), is an orchid plant found in various regions including Vietnam, Thailand, Laos, Myanmar, and South-Central China. The specific epithet "*falcata*" refers to its characteristic sickle-shaped structure.[10] *A. falcata* has several heterotypic synonyms such as *Aerides larpantae*, *Aerides mendelii*, *Aerides retrofracta*, and *Aerides siamensis*.[18] *A. falcata* has been used traditionally as a tonic for infants and wound healing for several skin diseases.[19] Despite its traditional use as a medicinal plant, no studies have explored its potential in treating CNS diseases or characterized its chemical composition. Hence, the present study aimed to identify the phytochemical constituents present in *A. falcata* extract and evaluate their efficacy in treating CNS diseases to discover potential bioactive leads.

Results and discussion

Structural characterization

Phytochemical investigation of EtOAc extract prepared from the aerial parts of *Aerides falcata* resulted in the purification of a novel compound (**1**), along with nine known compounds. The nine known compounds were identified as *n*-eicosyl-*trans*-ferulate (**2**),[20] denthyrsinin (**3**),[21] 2,4-dimethoxy-3,7-dihydroxyphenanthrene (**4**),[22] 2,7-dihydroxy-3,4,6-trimethoxyphenanthrene (**5**),[23] 3,7-dihydroxy-2,4,6-trimethoxyphenanthrene (**6**),[24] agrostonin (**7**),[25] paprazine (**8**),[26] syringaresinol (**9**)[27] and *n-trans*-feruloyl tyramine (**10**)[28] (Fig. 1B).

Compound **1** was purified as a brown amorphous solid. The molecular formula $C_{31}H_{24}O_8$ was analyzed by HR-ESI-MS with $[M - H]^-$ at *m*/*z* 523.1387 (calculated for $C_{31}H_{23}O_8$, 523.1392). The IR spectrum displayed absorption bands for hydroxyl groups (3384 cm^{-1}) and aromatic rings (2935, 1589 cm^{-1}). The UV absorptions exhibited the characteristic of phenanthrene nucleus at 265, 313, 353, and 371 nm.[29] The ^{13}C NMR spectrum showed 28 aromatic carbons were indicative of a dimeric phenanthrene structure. This was supported by the presence of two pairs of *ortho*-coupled doublets at δ 6.87 (1H, d, $J = 9.2$ Hz, H-10′), 6.94 (1H, d, $J = 8.8$ Hz, H-10), 7.32 (1H, d, $J = 9.2$ Hz, H-9′) and 7.36 (1H, d, $J = 8.8$ Hz, H-9) in the ^1H NMR spectrum. The ^1H and ^{13}C NMR resonances from one part of a phenanthrene unit (rings A, B, and C) of **1** showed similarity with agrostonin (**7**), a phenanthrene dimer with two identical units isolated from this plant. These included three singlet protons at 6.99 (1H, s, H-3), 7.20 (1H, s, H-8), and 9.25 (1H, s, H-5), together with two methoxy groups at 4.07 (3H, s, MeO-6) and 4.23 (3H, s, MeO-4). In the HMBC spectrum, C-9 (δ 127.9) showed correlation with H-8 and C-4a (δ 116.3) showed correlations with H-3

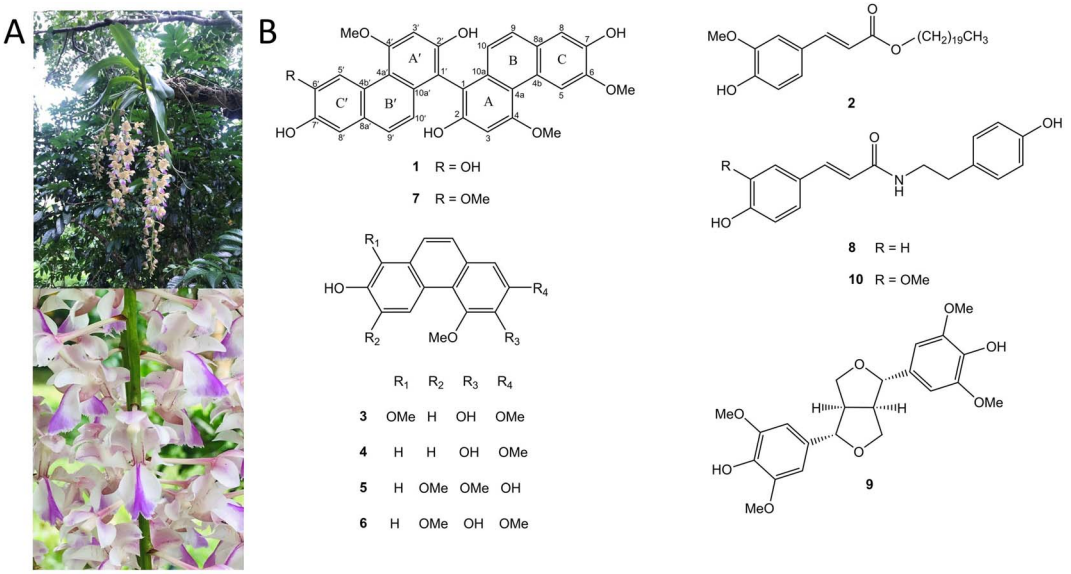

Fig. 1 (A) *Aerides falcata* (B) chemical structures of compounds **1–10**.

and H-5. The methoxy group at C-4 (δ 160.2) was confirmed by their NOESY correlations with H-3 and H-5. The methoxy group at C-6 (δ 148.4) was based on its NOESY cross-peak with H-5. The quaternary carbon of C-1 (δ 109.9) was assigned based on its three-bond correlations with H-3 and H-10. Comparison of ^{1}H and ^{13}C NMR of another phenanthrene unit (ring A′, B′ and C′) of **1** with those of agrostonin (**7**) revealed their structure similarity, except for the exhibition of a hydroxyl group at C-6′, instead of a methoxy group. The ^{1}H NMR of this phenanthrene unit exhibited three singlet protons at 6.96 (1H, s, H-3′), 7.19 (1H, s, H-8′), and 9.19 (1H, s, H-5′) and a methoxy group at δ 4.17 (3H, s, MeO-4′). The assignments of H-3′ and H-5′ were supported by their HMBC correlation with C-4a′ (δ 116.0). H-8′ was assigned by its HMBC correlation with C-9′ (δ 128.1).

The methoxy group was located at C-4′ according to its NOESY interaction with H-3′ and H-5′. The C-1′ (δ 109.6) of this phenanthrene unit showed 3-bond correlations with H-3′ and H-10′ in the HMBC spectrum. The two phenanthrene units were linked between C-1 and C-1′ based on the appearance of C-1 and C-1′ as non-oxygenated aromatic quaternary carbon, instead, they formed a C–C bond connecting the two monomers.[29] Based on the above spectral evidence, compound **1** was identified as a novel biphenanthrene derivative, and the trivial name aerifalcatin was given to the compound.

A comparison was made between the Electronic Circular Dichroism (ECD) spectra of M-bulbocodioidin E, which showed a positive Cotton effect around 250 nm and a negative Cotton effect around 350 nm, and P-bulbocodioidin E, which showed Cotton effects at the two wavelengths with opposite signs.[30] The experimental ECD spectrum of compound **1** (Fig. 2) showed a positive Cotton effect at 237 nm ($\Delta\varepsilon$ +9.0) and a negative Cotton effect at 331 nm ($\Delta\varepsilon$ −7.2), which was in agreement with P-bulbocodioidin E.[30] These observations suggest that the absolute configuration of this compound was the P-configuration.

Compounds **1** and **7** were likely formed through a process of oxidative coupling involving 2 monomers between aerosanthrene and/or 2,7-dihydro-4,6-dimethoxyphenanthrene, both of which are metabolites found in the plant.[31,32] One possible mechanism for this process is depicted in Fig. 3, which involves the removal of a hydrogen-free radical from the phenanthrene ring of 2,7-dihydro-4,6-dimethoxyphenanthrene at C-1 and C-1′ or aerosanthrene at C-1′.[33] This results in the linkage of the C-1′ of aerosanthrene to C-1 of 2,7-dihydro-4,6-dimethoxyphenanthrene forming compound **1**. In contrast, compound **7** is a linkage of two monomers of 2,7-dihydro-4,6-dimethoxyphenanthrene at C-1 and C-1′.

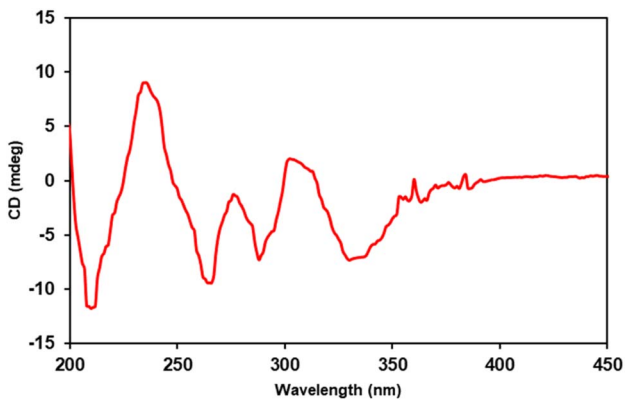

Fig. 2 The experimental ECD curve of **1**.

Constituents of *Aerides falcata* suppressed proinflammatory mediators in LPS-stimulated BV-2 microglial cells

Neuroinflammation is a fundamental aspect of CNS-associated diseases, including Parkinson, Alzheimer, multiple sclerosis, chronic pain, amyotrophic lateral sclerosis, and bacterial meningitis.[5–7] Microglia, which are the immune cells located in the CNS, play a role in the development and progression of neuroinflammation in CNS-related diseases.[34] Glial-modulating agents have been shown to be effective in improving patient outcomes.[35] In this research, we assessed the potential anti-neuroinflammatory activity of constituents of *Aerides falcata* using an *in vitro* model of neuroinflammation involving LPS-stimulated BV-2 cells. First, an MTT assay was used to determine safe concentrations of the compounds to

Table 1 ^{1}H (400 MHz) and ^{13}C-NMR (100 MHz) spectral data of **1** in acetone-d_6

Position	δ_H (multiplicity, J in Hz)	δ_C	HMBC (correlation with ^{1}H)
1	—	109.9	3, 10
2	—	155.0	3[a]
3	6.99 (s)	100.0	—
4	—	160.2	3[a], MeO-4
4a	—	116.3	3, 5, 10
4b	—	125.8	8, 9
5	9.25 (s)	109.7	—
6	—	148.4	5[a], 8, MeO-6
7	—	146.0	5, 8[a]
8	7.20 (s)	112.1	9
8a	—	128.0	5, 10
9	7.36 (d, 8.8)	127.9	8
10	6.94 (d, 8.8)	123.3	—
10a	—	135.4	9
1′	—	109.6	3′, 10′
2′	—	155.0	3′[a]
3′	6.96 (s)	99.7	—
4′	—	160.3	3′[a], MeO-4′
4a′	—	116.0	3′, 5′, 10′
4b′	—	126.2	8′, 9′
5′	9.19 (s)	113.5	—
6′	—	146.2	5′[a], 8′
7′	—	145.0	5′, 8′[a]
8′	7.19 (s)	112.4	9′
8a′	—	127.6	5′, 10′
9′	7.32 (d, 9.2)	128.1	8′
10′	6.87 (d, 9.2)	122.6	—
10a′	—	135.5	9′
MeO-4	4.23 (s)	56.1	—
MeO-6	4.07 (s)	56.0	—
MeO-4′	4.17 (s)	55.8	—

[a] Two-bond coupling.

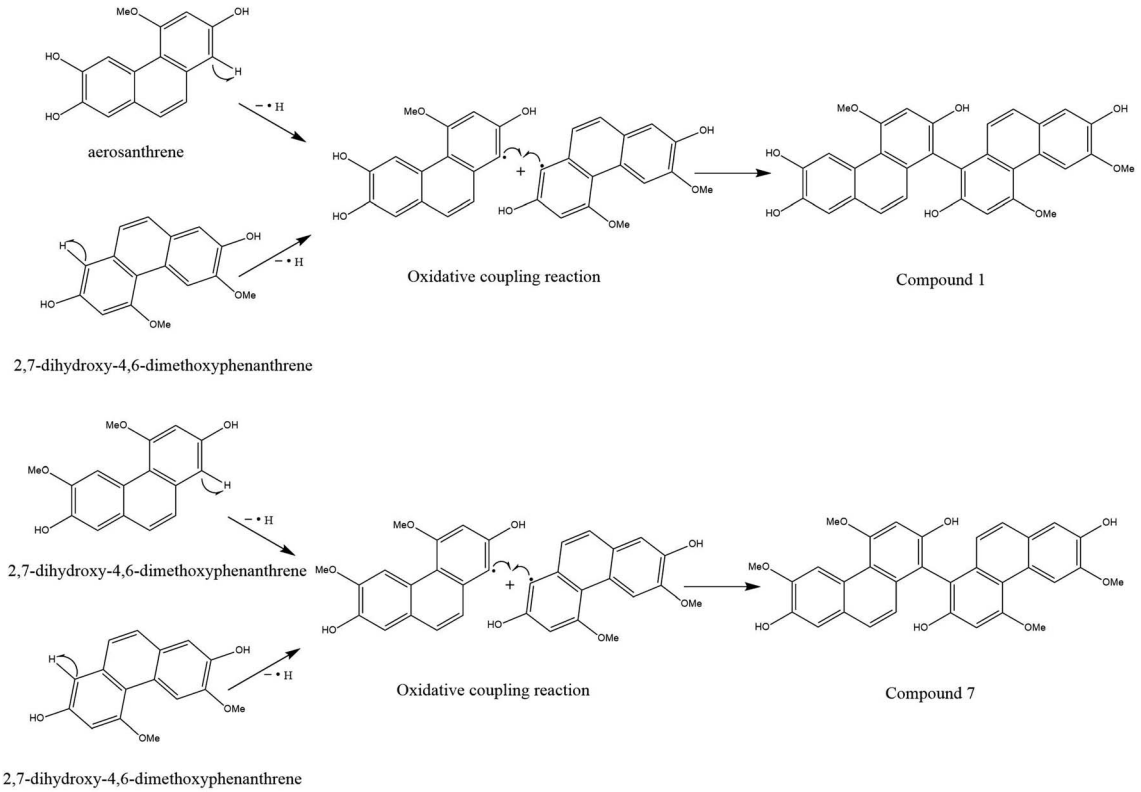

Fig. 3 Possible biogenetic pathway of compounds **1** and **7**.

Table 2 The effects of *Aerides falcata* constituents on LPS-stimulated NO release in BV-2 microglial cells

Compound	IC_{50} (mean ± SD) (μM)
1	0.87 ± 0.45
2	19.76 ± 1.36
3	8.99 ± 0.91
4	12.56 ± 1.30
5	2.47 ± 0.73
6	21.92 ± 3.70
7	2.55 ± 0.32
9	1.40 ± 0.17
10	18.62 ± 9.56
Minocycline	3.41 ± 0.30

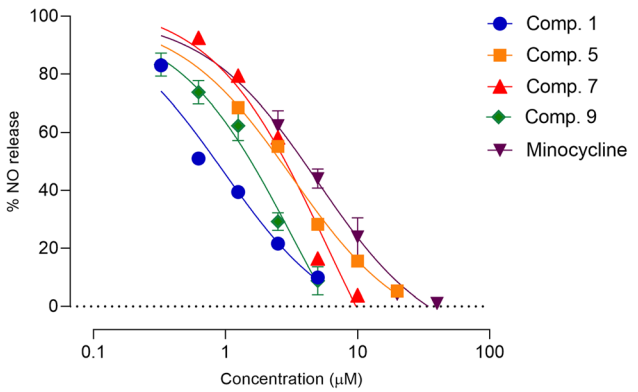

Fig. 4 Effects of compounds **1**, **5**, **7**, and **9** on LPS-induced NO production in BV-2 microglia cells. Each point on the graph represents mean ± SD (n = 3 independent experiments).

avoid false-positive results caused by toxicity (Table S10†). Subsequently, the safe concentrations of the test compounds were used to evaluate their anti-neuroinflammatory activity using NO and cytokine assays. As demonstrated in Table 2, compounds **1** and **9** exhibited greater NO release suppression activity compared to the reference compound, minocycline, whereas compounds **5** and **7** had similar activity. Moreover, the remaining compounds demonstrated lower NO-inhibitory activity than minocycline. The IC_{50} values of compounds **1**, **5**, **7**, **9**, and minocycline were 0.87 ± 0.45, 2.47 ± 0.73, 2.55 ± 0.32, 1.40 ± 0.17, and 3.41 ± 0.30 μM, respectively. Therefore, these compounds were further assessed in subsequent experiments (Fig. 4).

Pathological conditions featuring neuroinflammation are characterized by dysregulated and elevated levels of cytokines, including TNF-α, which contributes to its pathological role by increasing glutamate-mediated cytotoxicity.[36] IL-6, another inflammatory mediator, also contributes to the development and progression of CNS disorders. Modulating IL-6 release and its pathways have been shown to improve CNS disease conditions *in vivo*.[37] Thus, the effects of compounds **1**, **5**, **7**, and **9** on LPS-stimulated cytokine release in BV-2 microglial cells were further assessed. Results shown in Fig. 5 indicate that these

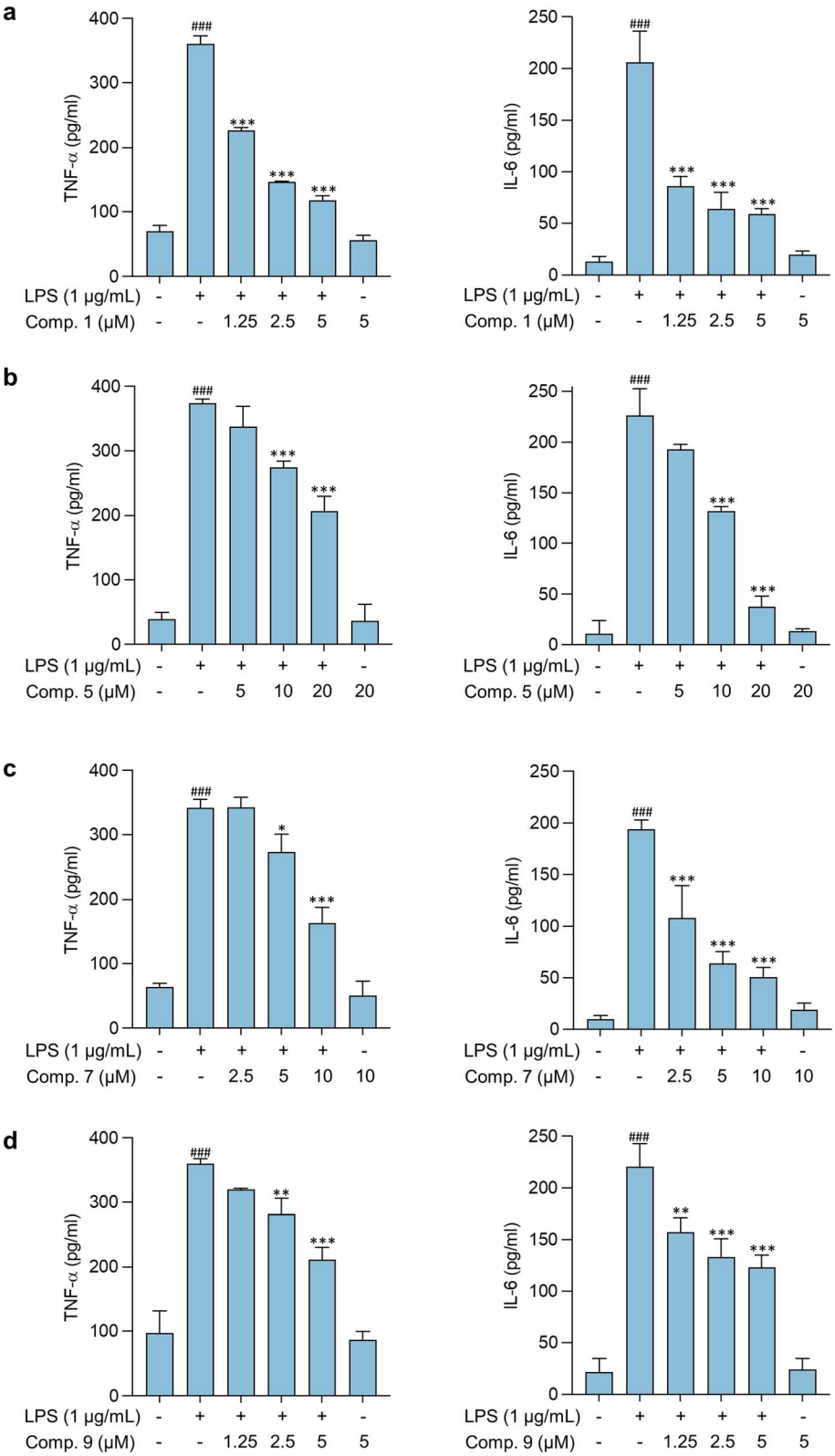

Fig. 5 Effects of compounds (a) **1**, (b) **5**, (c) **7**, and (d) **9** on cytokine release in LPS-stimulated BV-2 microglial cells. Data are presented as mean ± SD ($n = 3$ independent experiments). $^{###}p < 0.001$, control (0.5% DMSO) *vs.* LPS groups. $^{*}p < 0.05$, $^{**}p < 0.01$, $^{***}p < 0.001$, LPS *vs.* compound-treated groups. Statistical difference between groups was analyzed using one-way ANOVA followed by Bonferroni *post hoc* test.

Table 3 Cytotoxicity profiles of *Aerides falcata* constituents in C6 glioblastoma and SH-SY5Y cells

	IC_{50} (mean ± SD) (μM)	
Compound	C6 cells	SH-SY5Y cells
1	27.05 ± 2.21	29.21 ± 11.30
2	>160	>160
3	>160	>160
4	>160	>160
5	>160	>160
6	>160	>160
7	30.70 ± 8.58	92.28 ± 6.27
9	79.18 ± 20.29	126.11 ± 24.99
10	>160	>160

compounds significantly reduce the expression of proinflammatory cytokines, TNF-α, and IL-6 in activated microglia, suggesting their potential as anti-neuroinflammatory agents. Previous studies have also demonstrated the anti-inflammatory properties of compounds **5**, **7**, and **9**.[38,39] Compounds **5** and **7** were found as constituents of the rhizomes of *Bletilla formosana* (Hayata) Schltr. and showed potential anti-inflammatory activity by modulating neutrophils.[38] Furthermore, compound **9** alleviated inflammatory responses in activated macrophages and microglia.[38,39] However, this study is the first to report the anti-neuroinflammatory activity of compounds **1**, **5**, and **7** on activated microglia.

Constituents of *Aerides falcata* suppressed brain cancer cell growth and migration

Glioblastoma and primary central nervous system neuroblastoma (PCNSN) are malignant neoplasms that affect the central nervous system (CNS), characterized by their aggressive and fast-growing nature.[9,40] Various treatment modalities, such as surgery, radiotherapy, and chemotherapy, have been widely utilized in the clinical management of brain cancer. However, chemotherapy drugs have limited therapeutic efficacy and exhibit significant side effects, necessitating the development of novel therapeutic agents.[9,40] Hence, this study aimed to investigate the cytotoxic effects of *Aerides falcata* constituents in C6 glioblastoma and SH-SY5Y cells to evaluate their potential as a treatment option for brain cancer. The results of this study indicate that compounds **1**, **7**, and **9** possess potent cytotoxic activity in both C6 glioblastoma and SH-SY5Y cells, as demonstrated in Table 3 and Fig. 6. The IC_{50} values of compounds **1**, **7**, and **9** in C6 cells were found to be 27.05 ± 2.21, 30.70 ± 8.58, and 79.18 ± 20.29, respectively, as presented in Table 3. In SH-

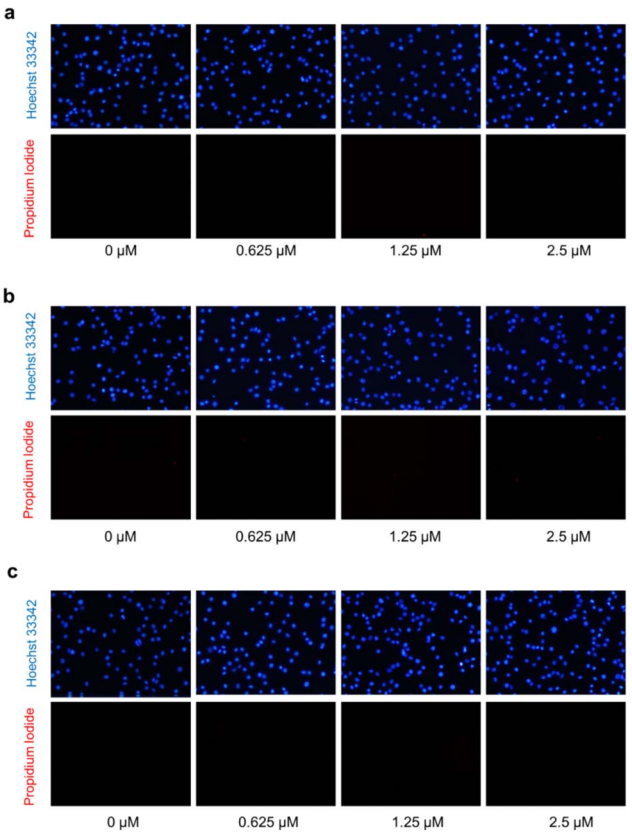

Fig. 7 Propidium iodide (PI) and Hoechst 33342 double staining in C6 glioblastoma cells after treatment with compounds **1** (a), **7** (b), and **9** (c) using fluorescence microscopy.

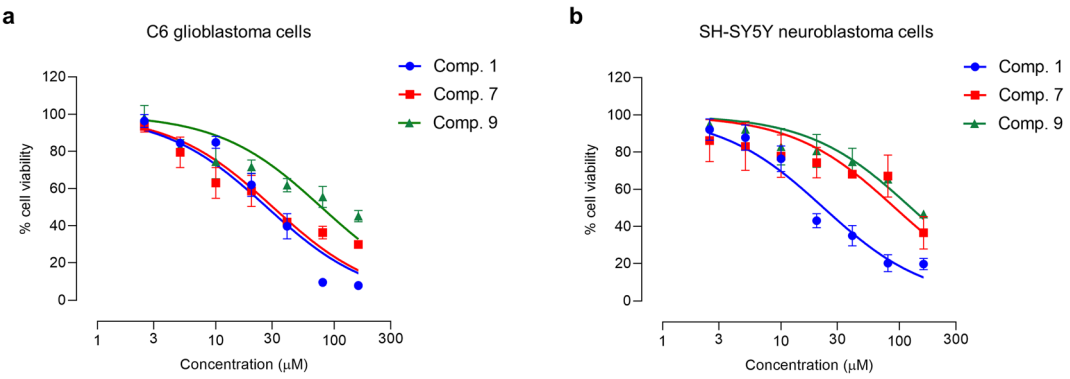

Fig. 6 Cytotoxicity profiles of compounds **1**, **7**, and **9** in (a) C6 glioblastoma and (b) SH-SY5Y neuroblastoma cells. Each point on the graph represents mean ± SD ($n = 3$ independent experiments).

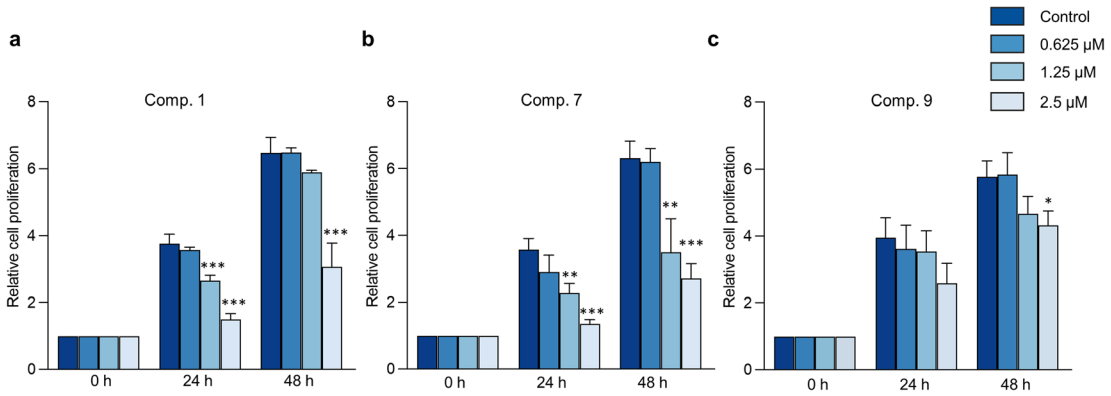

Fig. 8 The effects of *Aerides falcata* constituents on cell proliferation in C6 glioblastoma cells. Relative cell proliferation of C6 glioblastoma cells after being treated with compounds **1** (a), **7** (b), and **9** (c) at different concentrations (0, 0.625, 1.25, 2.5 μM). Bar graphs represent the relative cell proliferation expressed as mean ± SD ($n = 3$ independent experiments). *$p < 0.05$, **$p < 0.01$, ***$p < 0.001$, control *vs.* compound-treated groups. Statistically significant differences between groups were analyzed using one-way ANOVA followed by the Dunnett *post hoc* test.

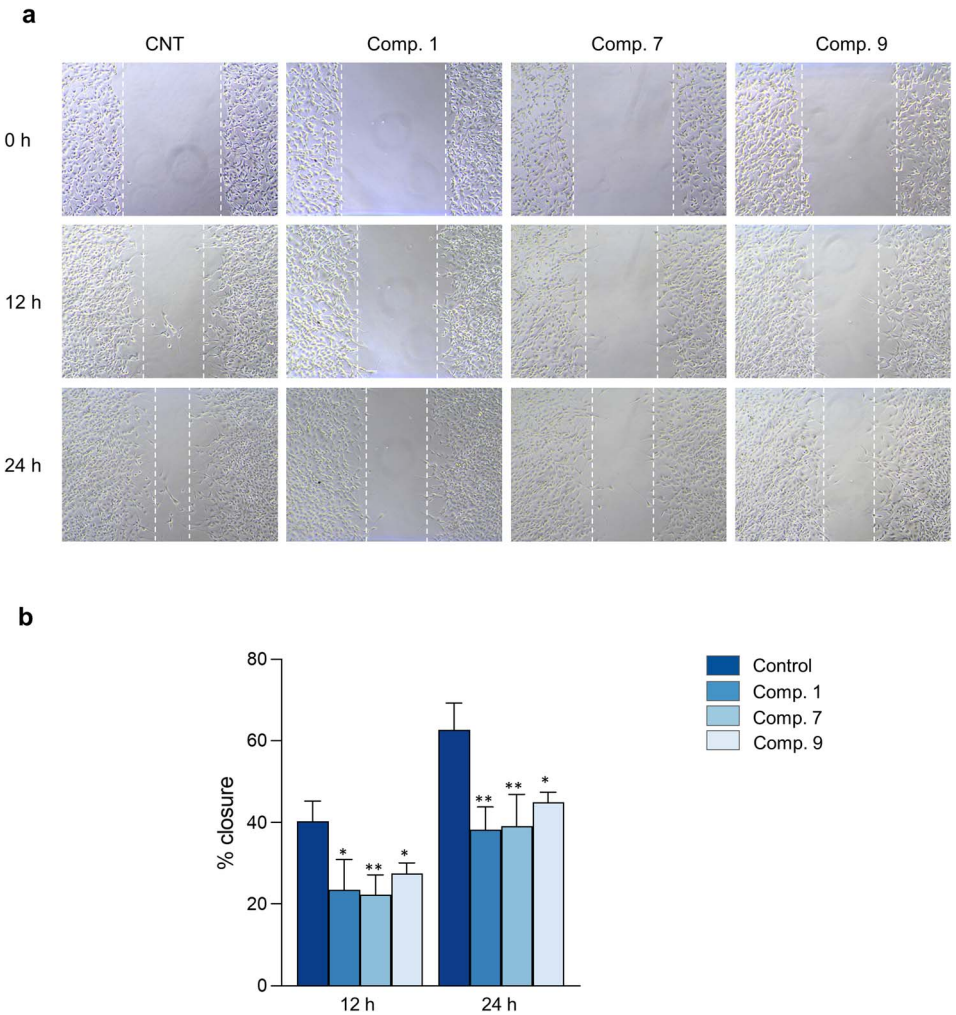

Fig. 9 The effects of *Aerides falcata* constituents on cell migration in C6 glioblastoma cells. Representative figures of the cell migration of C6 glioblastoma cells (a) and percentage of wound closure (b) after being treated with compounds **1**, **7**, and **9** at 2.5 μM concentration. Bar graphs represent the percentage of wound closure and are expressed as mean ± SD ($n = 3$ independent experiments). Statistical significance between groups was analyzed using one-way ANOVA followed by the Dunnett *post hoc* test. *$p < 0.05$ and **$p < 0.01$, control *vs.* compound-treated groups.

SY5Y cells, the IC_{50} values of compounds **1**, **7**, and **9** were found to be 29.21 ± 11.30, 92.28 ± 6.27, and 126.11 ± 24.99 μM, respectively. Moreover, the impact of compounds **1**, **7**, and **9** on the behavior of cancer cells was also examined.

The hallmark of brain cancer, such as glioblastoma, is its high growth rate and invasive potential into the surrounding tissue.[41] As a result, it is crucial to curb the proliferation and migration of cancer cells to adjacent tissues. In this study, we evaluated the impact of compounds **1**, **7**, and **9** on cell proliferation and migration in C6 cells. We first determined the safe concentrations of the test compounds *via* Hoechst 33342/PI double staining assay, which demonstrated no significant induction of cellular death (necrosis and apoptosis) at 0.625, 1.25, and 2.5 μM concentrations compared to the control, as depicted in Fig. 7 and Table S11.† These safe concentrations were used to evaluate the effects of the test compounds on cell proliferation and migration. As illustrated in Fig. 8, compounds **1**, **7**, and **9** significantly inhibited cell proliferation at 24 and 48 h post-treatment. Moreover, compounds **1**, **7**, and **9** inhibited cell migration in a concentration-dependent manner, as evidenced by the decrease in the wound area (Fig. 9). Notably, previous studies have also reported anticancer effects of compound **9** in prostate cancer,[42] leukemia,[43] and breast cancer.[44] To the best of our knowledge, this is the first investigation into the suppressive role of compounds **1**, **7**, and **9** in brain cancer cells.

Experimental

General experimental procedures of chemical characterization

NMR spectra were obtained using a Bruker Avance Neo 400 MHz NMR spectrometer (Billerica, MA, USA). Mass spectra were recorded on a Bruker micro TOF mass spectrometer (ESI-TOF-MS) (Billerica, MA, USA). Optical rotation was obtained using Jasco p-2000 digital polarimeter (Easton, MD, USA). The ECD spectra were calculated by JASCO J-810. UV spectra were measured using a Milton Roy Spectronic 3000 Array spectrophotometer (Rochester, Monroe, NY, USA). IR spectra were determined with a PerkinElmer FT-IR 1760X spectrophotometer (Boston, MA, USA). Semi-preparative HPLC was performed using the Shimadzu HPLC (Kyoto, Japan).

Plant material

The samples of *Aerides falcata* were purchased from the Chatuchak market in February 2021. Authentication was performed by Mr Yanyong Punpreuk, Department of Agriculture, Bangkok, Thailand. A voucher specimen BS-AF-022564 was deposited at the Department of Pharmacognosy and Pharmaceutical Botany, Faculty of Pharmaceutical Sciences, Chulalongkorn University, Thailand.

Extraction and isolation

The dried and powdered aerial parts of *Aerides falcata* (2.0 kg) were macerated with MeOH (3 × 15 L) to give a MeOH extract after evaporating the solvent. The MeOH extract (105.0 g) was fractionated by solvent partition using EtOAc, butanol, and water to obtain EtOAc (20.4 g), butanol (48.9 g), and aqueous (28.1 g) extracts, respectively. The EtOAc extract was initially separated by vacuum-liquid chromatography on silica gel (EtOAc/hexane, gradient) to give 7 fractions (A to G). Fraction C (7.1 g) was isolated by Sephadex LH-20 and then by column chromatography (CC, silica gel, CH_2Cl_2/hexane, gradient) and CC (silica gel, EtOAc/hexane, 1 : 9), respectively, to yield *n*-eicosyl-*trans*-ferulate (**2**) (36 mg). Fraction D (3.8 g) was fractionated by Sephadex LH-20 (acetone) and then by CC (silica gel, CH_2Cl_2/hexane, gradient) to give 5 fractions (D-I to D-V). Denthyrsinin (**3**) (7 mg) was obtained from fraction D-II. Fraction D-IV (23 mg) was purified by CC (silica gel, EtOAc/hexane, gradient) to afford 2,4-dimethoxy-3,7-dihydroxyphenanthrene (**4**) (10 mg). 2,7-Dihydroxy-3,4,6-trimethoxyphenanthrene (**5**) (7 mg) was yielded from fraction D-V (21 mg) after purification by CC (silica gel, EtOAc/hexane, gradient). Fraction E (2.2 g) was separated on Sephadex LH-20 (MeOH) to give 6 fractions (E-I to E-VI). Fraction E-III (60 mg) was isolated by CC (silica gel, EtOAc/hexane, gradient), and after that, repeated CC in the same manner to furnish 3,7-dihydroxy-2,4,6-trimethoxyphenanthrene (**6**) (3 mg). Fraction F (6.6 g) was separated by Sephadex LH-20 (MeOH) to give 7 fractions (F-I to F-VII). Fraction F-IV (87 mg) was purified by CC (silica gel, acetone/hexane, gradient) to yield agrostonin (**7**) (58 mg). Fraction F-V (98 mg) was subjected to CC (silica gel, MeOH/CH_2Cl_2, 5 : 95) to obtain 4 fractions (F-Va to F-Vd). Compound **1** (11 mg) was obtained from fraction F-Vb (15 mg) after purification by preparative thin-layer chromatography (silica gel, EtOAc/hexane, 2 : 8). Fraction F-Vc (20 mg) was isolated by semi-preparative HPLC (silica gel, MeOH/CH_2Cl_2, 5 : 95) to yield paprazine (**8**) (1 mg). Fraction G (10.7 g) was separated by CC (silica gel, EtOAc/CH_2Cl_2, gradient) and then subjected to repeat CC (silica gel, MeOH/CH_2Cl_2, 3 : 97) to furnish syringaresinol (**9**) (7 mg) and *n-trans*-feruloyl tyramine (**10**) (2 mg), respectively.

Aerifalcatin (**1**) brown amorphous solid; $[\alpha]_D^{25}$ −20 (*c* 0.6, MeOH); ECD (MeOH) λ_{max} ($\Delta\varepsilon$) 237 (+9.0), 266 (−9.4), 288 (−7.3), 302 (+2.0), 331 (−7.2) nm (Fig. 2); UV (MeOH) λ_{max} ($\log\varepsilon$) 265 (4.33), 313 (3.50), 353 (3.30), 371 (3.44); IR: ν_{max} 3384, 2935, 2850, 1704, 1589, 1543, 1475, 1266 cm^{-1}; HR-ESI-MS: $[M - H]^-$ at *m*/*z* 523.1387 (calcd for $C_{31}H_{23}O_8$, 523.1392); ^1H NMR (400 MHz, acetone-d_6) and ^{13}C NMR (125 MHz, acetone-d_6) (Table 1).

Cell culture

BV-2 microglial cells were purchased from AcceGen Biotechnology (Fairfield, NJ, USA), and SH-SY5Y neuroblastoma cells and C6 glioblastoma cells were purchased from ATCC (American Type Culture Collection) (Manassas, VA, USA). The cells were cultured, supplemented, and maintained following the manufacturer's instructions. The cell culture materials, including Dulbecco's Modified Eagle Medium (DMEM) and fetal bovine serum (FBS), were purchased from PAN Biotech (Aidenbach, Germany). DMEM-F12 and penicillin/streptomycin were purchased from Gibco, Thermo Fisher Scientific, Inc. (Waltham, MA, USA). Lipopolysaccharide (LPS), an inducer of

inflammatory responses, and minocycline, a reference compound for anti-neuroinflammatory activity, were purchased from Sigma-Aldrich (St. Louis, MO, USA).

Cell treatment

Nine out of ten compounds (compounds **1–7** and **9–10**) were evaluated in CNS disease models due to the limited amount of compound **8**. LPS-induced BV-2 microglial cells were used as a model of neuroinflammation. Initially, the cell viability assay was performed to determine the non-toxic concentrations of the test compounds. Briefly, the cells were seeded in 96 well plates at a density of 2×10^4 cells per well for 24 h, followed by the cell viability assay. After that, the safety concentrations were used to perform NO and cytokine assays. Briefly, the cells were seeded in 48-well plates at a density of 7.5×10^4 cells per well for 24 h. The cells were then treated with the test compounds for 2 h and co-incubated with LPS for another 22 h. The media were collected and further used for NO and cytokine assays.

SH-SY5Y neuroblastoma cells and C6 glioblastoma cells were used as brain cancer models. Cytotoxicity assay was performed in both cells using MTT assay. Briefly, SH-SY5Y and C6 cells were seeded in 96 well plates at a density of 5×10^4 cells per well and 2×10^4 cells per well, respectively. After 24 h, the cells were exposed to different concentrations of test compounds (0, 2.5, 5, 10, 20, 40, 80, and 160 μM) for another 24 h. The cell viability assay was then performed to determine the cytotoxicity levels of the compounds. Furthermore, Hoechst 33342/propidium iodide staining assay was performed to assess the safety concentrations of the test compounds. The safety concentrations were further used in cell proliferation and cell-scratch assay models to determine the cancerous behaviors of the cells.

Cell viability assay

The cell viability was determined using the MTT assay (Sigma-Aldrich, St. Louis, MO, USA). Briefly, after cell treatment, the media in multi-well plates were removed and washed, followed by the addition of MTT solution (0.5 mg mL^{-1}). After 3 h, the formazan crystals were dissolved with DMSO (Sigma-Aldrich, St. Louis, MO, USA). The absorbance was measured under a microplate reader (BMG Labtech, Ortenberg, Germany) at 570 nm maximum wavelength.

NO assay

The NO assay reagents were prepared according to the manufacturer's instructions (Sigma-Aldrich, St. Louis, MO, USA). After cell treatment, 100 μL of culture media was collected and placed into 96 well plates. The collected media was added with 100 μL of Griess reagent and incubated for 20 min in the dark. The absorbance was measured using a microplate reader at 520 nm.

ELISA assay

TNF-α and IL-6 levels in the cell culture media after cell treatments were analyzed using ELISA assay. The assay was performed according to the protocol provided by the manufacturer (BioLegend, San Diego, CA, USA).

Hoechst 33342/propidium iodide (PI) assay

Hoechst 33342/PI staining (Sigma-Aldrich, St. Louis, MO, USA) was performed to confirm the safety concentrations of the test compounds in the cells. Briefly, the cells were seeded in 48 well plates at a density of 5×10^4 cells per well for 24 h. The cells were treated with the test compounds at concentrations of 0.625, 1.25, and 2.5 μM for another 24 h. Then the cells were exposed to a solution of Hoechst 33342/PI for 20 min. The cells were then visualized under a fluorescence microscope (Olympus IX51 inverted microscope, Tokyo, Japan).

Cell proliferation assay

The ability of the test compounds to suppress cancer cell proliferation was assessed using the MTT assay. Briefly, the cells were seeded in 96 well plates with a density of 5×10^3 for 24 h. The cells were then treated with the test compounds, and the cell proliferation was assessed at 0, 24, and 48 h post-compound treatment.

Cell scratch assay

Cell scratch assay was performed to assess the effects of compounds on the migration of the cancer cells. Briefly, the cells were seeded in 24 well plates at a density of 1.5×10^5 for 24 h. The cells were then scratched with a 200 μl pipette tip (Corning Inc., Corning, NY, USA) to generate a wound area. The floating cells were removed by rinsing them with PBS. The wound of the cells was then visualized and captured under a microscope at 0, 12, and 24 h post-compound treatment.

Statistical analysis

The data were presented as mean ± SD. The statistical analysis and visualization of data were performed using GraphPad prism. IC_{50} values were determined using non-linear regression. The statistical differences between groups were analyzed using One-way ANOVA followed by Dunnett's or Bonferroni *post hoc* analyses.

Conclusions

In summary, we demonstrate the potential of chemical constituents isolated from *Aerides falcata* in ameliorating neuroinflammation and reducing cytotoxicity. A novel compound **1** and nine known compounds were isolated and purified from the plant extract. The *in vitro* model of neuroinflammation utilizing LPS-stimulated BV-2 cells was employed to assess the anti-neuroinflammatory activity of the isolated compounds. The findings demonstrated that compounds **1**, **5**, **7**, and **9** exhibited significant anti-neuroinflammatory effects by suppressing the expression of proinflammatory cytokines, TNF-α and IL-6, in activated microglia. Furthermore, the isolated compounds **1**, **7**, and **9** were observed to exert potent cytotoxic activity in C6 glioblastoma and SH-SY5Y cells. Overall, the study

highlights the potential of *Aerides falcata* constituents as promising anti-neuroinflammatory and cytotoxic agents, thereby offering potential therapeutic benefits in the treatment of central nervous system diseases and brain cancer.

Author contributions

Conceptualization, P. R., P. T. and B. S; data curation, B. R., H., P. W. D. W. and B. S.; formal analysis, B. R., H., P. W. D. W., P. R., P. T. and B. S.; investigation, B. R., H., P. W. D. W., C. C. and B. S.; methodology, B. R., H., P. W. D. W., P. R., P. T., K. L. and B. S.; resources, Y. P. and B. S.; supervision, P. R., P. T. and B. S.; writing – original draft, B. R., H. and B. S.; writing – review & editing, P. R., P. T. and B. S.

Conflicts of interest

The authors declare no conflict of interest.

Acknowledgements

This work was supported by the 90th Anniversary of Chulalongkorn University Fund (Ratchadaphiseksomphot Endowment Fund). We are grateful to Dr Waraluck Chaichompoo from the Department of Food and Pharmaceutical Chemistry, Faculty of Pharmaceutical Sciences, Chulalongkorn University, Bangkok, 10330, Thailand, for her assistance with the ECD measurements and valuable discussions. B. R. thanks the Graduate School, Chulalongkorn University, for a CU-ASEAN scholarship.

References

1 A. S. Winkler, The growing burden of neurological disorders in low-income and middle-income countries: priorities for policy making, *Lancet Neurol.*, 2020, **19**, 200–202.
2 D. C. Bergen and D. Silberberg, Nervous system disorders: A global epidemic, *Arch. Neurol.*, 2002, **59**, 1194.
3 D. E. Pankevich, B. M. Altevogt, J. Dunlop, F. H. Gage and S. E. Hyman, Improving and accelerating drug development for nervous system disorders, *Neuron*, 2014, **84**, 546–553.
4 J. C. DiNunzio and R. O. Williams III, CNS disorders—current treatment options and the prospects for advanced therapies, *Drug Dev. Ind. Pharm.*, 2008, **34**, 1141–1167.
5 D. Erny, A. L. Hrabě de Angelis, D. Jaitin, P. Wieghofer, O. Staszewski, E. David, H. Keren-Shaul, T. Mahlakoiv, K. Jakobshagen, T. Buch, V. Schwierzeck, O. Utermöhlen, E. Chun, W. S. Garrett, K. D. McCoy, A. Diefenbach, P. Staeheli, B. Stecher, I. Amit and M. Prinz, Host microbiota constantly control maturation and function of microglia in the CNS, *Nat. Neurosci.*, 2015, **18**, 965–977.
6 R.-R. Ji, Z.-Z. Xu and Y.-J. Gao, Emerging targets in neuroinflammation-driven chronic pain, *Nat. Rev. Drug Discovery*, 2014, **13**, 533–548.
7 P. Agyeman, D. Grandgirard and S. L. Leib, Neuroinflammation in bacterial meningitis in *The blood–brain barrier and inflammation*, ed. R. Lyck and G. Enzmann, Springer, Switzerland, 2017, pp. 213–252.
8 G. Minniti, R. Muni, G. Lanzetta, P. Marchetti and R. M. Enrici, Chemotherapy for glioblastoma: Current treatment and future perspectives for cytotoxic and targeted agents, *Anticancer Res.*, 2009, **29**, 5171–5184.
9 X. Lu, X. Zhang, X. Deng, Z. Yang, X. Shen, H. Sheng, B. Yin, N. Zhang and J. Lin, Incidence, treatment, and survival in primary central nervous system neuroblastoma, *World Neurosurg.*, 2020, **140**, e61–e72.
10 E. S. Teoh, *Medicinal orchids of Asia*, Springer, Singapore, 2016.
11 M. M. Hossain, Therapeutic orchids: traditional uses and recent advances—an overview, *Fitoterapia*, 2011, **82**, 102.
12 D. Li, G. Wang, Q. Wu, J. Shi and F. Zhang, *Dendrobium nobile* Lindl alkaloid attenuates 6-OHDA-induced dopamine neurotoxicity, *Biotechnol. Appl. Biochem.*, 2021, **68**, 1501–1507.
13 S. Yang, Q. Gong, Q. Wu, F. Li, Y. Lu and J. Shi, Alkaloids enriched extract from *Dendrobium nobile* Lindl. attenuates tau protein hyperphosphorylation and apoptosis induced by lipopolysaccharide in rat brain, *Phytomedicine*, 2014, **21**, 712–716.
14 Hasriadi, P. W. D. Wasana, B. Sritularak, O. Vajragupta, P. Rojsitthisak and P. Towiwat, Batatasin III, a Constituent of *Dendrobium scabrilingue*, Improves Murine Pain-like Behaviors with a Favorable CNS Safety Profile, *J. Nat. Prod.*, 2022, **85**, 1816–1825.
15 A. Lu, Y. Jiang, J. Wu, D. Tan, L. Qin, Y. Lu, Y. Qian, C. Bai, J. Yang, H. Ling, J. Shi, Z. Yang and Y. He, Opposite trends of glycosides and alkaloids in *Dendrobium nobile* of different age based on UPLC-Q/TOF-MS combined with multivariate statistical analyses, *Phytochem. Anal.*, 2022, **33**, 619–634.
16 K. Serter, M. Seçme and L. Elmas, Erianin, a promising agent in the treatment of glioblastoma multiforme triggers apoptosis in U373 and A172 glioblastoma cells, *Arch. Biol. Sci.*, 2022, **74**, 227–234.
17 S. Sut, F. Maggi and S. Dall'Acqua, Bioactive secondary metabolites from orchids (Orchidaceae), *Chem. Biodiversity*, 2017, **14**, e1700172.
18 M. J. Smith, C. Brodie, J. Kowalczyk, S. Michnowicz, H. N. McGough and J. A. Roberts, *CITES Orchid Checklist Volume 4 for the genera: Aerides, Coelogyne, Comparettia and Masdevallia*, The Royal Botanic Garden, London, 2016.
19 L. J. Lawler, Ethnobotany of the Orchidaceae, *Orchid biology review and perspectives*, ed. J. Ardithi, Cornell University Press, Ithaca, 1984, vol. 4, pp. 27–149.
20 H. T. San, P. Boonsnongcheep, W. Putalun, W. Mekboonsonglarp, B. Sritularak and K. Likhitwitayawuid, α-Glucosidase inhibitory and glucose uptake stimulatory effects of phenolic compounds from *Dendrobium christyanum*, *Nat. Prod. Commun.*, 2020, **15**, 1–8.
21 G.-N. Zhang, L.-Y. Zhong, S. W. Annie Bligh, Y.-L. Guo, C.-F. Zhang, M. Zhang, Z.-T. Wang and L.-S. Xu, Bi-bicyclic and bi-tricyclic compounds from *Dendrobium thyrsiflorum*, *Phytochemistry*, 2005, **66**, 1113–1120.

22 M. Yamaki and C. Honda, The stilbenoids from *Dendrobium plicatile*, *Phytochemistry*, 1996, **43**, 207–208.
23 P. L. Majumder and S. Pal (Née Ray), Rotundatin, a new 9,10-didydrophenanthrene derivative from *Dendrobium rotundatum*, *Phytochemistry*, 1992, **31**, 3225–3228.
24 Y. Chen, J.-J. Xu, H. Yu, C. Qing, Y.-L. Zhang, Y. Liu and J.-H. Wang, 3,7-Dihydroxy-2,4,6-trimethoxyphenanthrene, a new phenanthrene from *Bulbophyllum Odoratissimum*, *J. Chem. Soc.*, 2007, **51**, 352–355.
25 P. L. Majumder, S. Banerjee, S. Lahiri, N. Mukhoti and S. Sen, Dimeric phenanthrenes from two *Agrostophyllum* species, *Phytochemistry*, 1998, **47**, 855–860.
26 Atta-ur-Rahman, M. K. Bhatti, F. Akhtar and M. I. Choudhary, Alkaloids of *Fumaria indica*, *Phytochemistry*, 1992, **31**, 2869–2872.
27 B. P. Hyun, H. L. Kyu, H. K. Ki, K. L. Il, J. N. Hyung, U. C. Sang and R. L. Kang, Lignans from the roots of *Berberis amurensis*, *Nat. Prod. Sci.*, 2009, **15**, 17–21.
28 G. J. Kim, S. Park, E. Kim, H. Kwon, H.-J. Park, J.-W. Nam, S.-S. Roh and H. Choi, Antioxidant, pancreatic lipase inhibitory, and tyrosinase inhibitory activities of extracts of the invasive plant *Spartina anglica* (Cord-grass), *Antioxidants*, 2021, **10**, 242.
29 M. T. Thant, B. Sritularak, N. Chatsumpun, W. Mekboonsonglarp, Y. Punpreuk and K. Likhitwitayawuid, Three novel biphenanthrene derivatives and a new phenylpropanoid ester from *Aerides multiflora* and their α-glucosidase inhibitory activity, *Plants*, 2021, **10**, 385.
30 C. Wang, S. Shao, S. Han and S. Li, Atropisomeric bi(9,10-dihydro)phenanthrene and phenanthrene/bibenzyl dimers with cytotoxic activity from the pseudobulbs of *Pleione bulbocodioides*, *Fitoterapia*, 2019, **138**, 104313.
31 V. Cakova, A. Urbain, C. Antheaume, N. Rimlinger, P. Wehrung, F. Bonté and A. Lobstein, Identification of phenanthrene derivatives in *Aerides rosea* (Orchidaceae) using the combined system HPLC-ESI-HRMS/MS and HPLC-DAD-MS-SPE-UV-NMR, *Phytochem. Anal.*, 2015, **26**, 34–39.
32 J. S. Lim, D. Hahn, M. J. Gu, J. Oh, J. S. Lee and J. Kim, Anti-inflammatory and antioxidant effects of 2,7-dihydroxy-4,6-dimethoxy phenanthrene isolated from *Dioscorea batatas* Dence, *Appl. Biol. Chem.*, 2019, **62**(29), 35.
33 W. Ma, F. Liu, Y. Y. Ding, Y. Zhang and N. Li, Four new phenanthrenoid dimers from *Juncus effusus L.* with cytotoxic and anti-inflammatory activities, *Fitoterapia*, 2015, **105**, 83–88.
34 Y. S. Kim and T. H. Joh, Microglia, major player in the brain inflammation: Their roles in the pathogenesis of Parkinson's disease, *Exp. Mol. Med.*, 2006, **38**, 333–347.
35 Z. Alshelh, E. Mills, D. Kosanovic, F. di Pietro, P. Macey, E. R. Vickers and L. A. Henderson, Effects of the glial modulator palmitoylethanolamide on chronic pain intensity and brain function, *J. Pain Res.*, 2019, **12**, 2427–2439.
36 B. Becher, S. Spath and J. Goverman, Cytokine networks in neuroinflammation, *Nat. Rev. Immunol.*, 2017, **17**, 49–59.
37 M. Rothaug, C. Becker-Pauly and S. Rose-John, The role of interleukin-6 signaling in nervous tissue, *Biochim. Biophys. Acta*, 2016, **1863**, 1218–1227.
38 V. K. Bajpai, M. B. Alam, K. T. Quan, M.-K. Ju, R. Majumder, S. Shukla, Y. S. Huh, M. Na, S. H. Lee and Y.-K. Han, Attenuation of inflammatory responses by (+)-syringaresinol *via* MAP-Kinase-mediated suppression of NF-κB signaling *in vitro* and *in vivo*, *Sci. Rep.*, 2018, **8**, 9216.
39 L. Zhang, X. Jiang, J. Zhang, H. Gao, L. Yang, D. Li, Q. Zhang, B. Wang, L. Cui and X. Wang, (−)-Syringaresinol suppressed LPS-induced microglia activation *via* downregulation of NF-κB p65 signaling and interaction with ERβ, *Int. Immunopharmacol.*, 2021, **99**, 107986.
40 A. C. Tan, D. M. Ashley, G. Y. López, M. Malinzak, H. S. Friedman and M. Khasraw, Management of glioblastoma: State of the art and future directions, *CA-Cancer J. Clin.*, 2020, **70**, 299–312.
41 H. Schättler, U. Ledzewicz, Y. Kim, A. De Los Reyes and E. Jung, On the control of cell migration and proliferation in glioblastoma, in *Proceedings of the IEEE Conference on Decision and Control*, 2013, pp. 1810–1815.
42 D. Selvaraj, S. Muthu, S. Kotha, R. S. Siddamsetty, S. Andavar and S. Jayaraman, Syringaresinol as a novel androgen receptor antagonist against wild and mutant androgen receptors for the treatment of castration-resistant prostate cancer: molecular docking, *in vitro* and molecular dynamics study, *J. Biomol. Struct. Dyn.*, 2021, **39**, 621–634.
43 B.-Y. Park, S.-R. Oh, K.-S. Ahn, O.-K. Kwon and H.-K. Lee, (-)-Syringaresinol inhibits proliferation of human promyelocytic HL-60 leukemia cells *via* G1 arrest and apoptosis, *Int. Immunopharmacol.*, 2008, **8**, 967–973.
44 Y. H. Jeong, S. Y. Chung, A.-R. Han, M. K. Sung, D. S. Jang, J. Lee, Y. Kwon, H. J. Lee and E.-K. Seo, P-glycoprotein inhibitory activity of two phenolic compounds, (-)-syringaresinol and tricin from *Sasa borealis*, *Chem. Biodiversity*, 2007, **4**, 12–16.